Neural Changes in Patients with Post-Traumatic Anosmia: Insights from Resting-State fMRI

Abolhasan Rezaeyan (PhD)[1], Fatemeh Shahi Moridi (MSc)[2], Seyed Kamran Kamrava (MD)[3], Mohammad Bagher Shiran (PhD)[2], Arash Zare-Sadeghi (PhD)[2]*

[1]Cellular and Molecular Gerash Research Center, Gerash University of Medical Sciences, Gerash, Iran
[2]Finetech in Medicine Research Center, Medical Physics Department, School of Medicine, Iran University of Medical Sciences, Tehran, Iran
[3]ENT Research Center, Institute of Five Senses, Hazrat Rasoul Hospital, Iran University of Medical Sciences, Tehran, Iran

ABSTRACT

Background: Functional Magnetic Resonance Imaging (fMRI) is a powerful modality for investigating changes in healthy brains and those with disorders. Anosmia, an olfactory disorder, is commonly associated with traumatic brain injury, particularly in patients suffering from severe trauma.

Objective: In this study, we aimed to utilize Resting-State fMRI (rs-fMRI) to examine changes in Functional Connectivity (FC) networks between Healthy Controls (HCs) and patients with Post-Traumatic Anosmia (PTA).

Material and Methods: In this retrospective study, we performed rs-fMRI on forty-four PTA patients and forty-three HCs. The Sniffin' Sticks test was used to assess olfactory function. Seed-based Analysis (SBA) and Independent Component Analysis (ICA) were conducted using MATLAB-based imaging software.

Results: PTA patients showed lower Threshold-Discrimination-Identification (TDI) scores compared to HCs. SBA revealed increased FC correlations in the anterior cingulate cortex, piriform, insular cortex, and prefrontal area in PTA patients. Using ICA on the whole brain network, we found increased FC in the right frontal pole, cerebellum, right putamen, anterior cingulate cortex, postcentral gyrus, orbitofrontal cortex, and amygdala in PTA compared to HCs. In PTA patients, global efficiency of the entire brain network showed a significant association with olfactory performance.

Conclusion: This study suggests that neural-level olfactory deficits following head trauma are most accurately characterized through SBA and ICA analyses in higher-order regions outside the primary olfactory cortex.

Keywords

Anosmia; Functional MRI; Brain Mapping; Functional Connectivity; Olfactory Cortex

Introduction

The sense of smell plays a significant role in our daily lives. Changes in the detection (i.e., anosmia, hyposmia) or recognition (i.e., parosmia, phantosmia) of smells are typically experienced by individuals suffering from olfactory disorders [1]. Anosmia, the partial or complete loss of smell, can be caused by several factors, one of which is traumatic brain injury. Post-Traumatic Anosmia (PTA) is a common disorder affecting approximately 5-14.5% of individuals with head injuries [2]. Damage to the olfactory system can occur anywhere along the olfactory tract, from the nasal cavity to the brain [3]. PTA

*Corresponding author:
Arash Zare-Sadeghi
Finetech in Medicine Research Center, Medical Physics Department, School of Medicine, Iran University of Medical Sciences, Tehran, Iran
E-mail:
akcarash@gmail.com

Received: 27 May 2025
Accepted: 27 April 2026

is primarily evaluated using a psychophysical olfactory function test, which heavily relies on patient self-reporting [4]. However, the semi-objective nature of this psychophysical test can impact the diagnostic accuracy due to olfactory loss, impaired odor memory, and cognitive decline. Therefore, given the limitations of self-reporting, objective imaging provides a valuable tool for evaluating and diagnosing olfactory system disorders [5].

The Functional Magnetic Resonance Imaging (fMRI) provides a non-invasive technique for visualizing and assessing brain activity in humans, utilizing the measurement of Blood Oxygenation Level Dependent (BOLD) signals to enhance our basic understanding of the functioning of the olfactory system [6]. Essentially, fMRI provides fundamental insights into the workings of the olfactory system by assessing the Functional Connectivity (FC) of the brain. Consequently, fMRI data are instrumental in predicting olfactory disorders and enhancing treatment methodologies [7]. Nevertheless, task-based fMRI can be difficult to implement in patients with olfactory dysfunction, largely because of cognitive deficits that frequently accompany the condition. Furthermore, the outcomes of task-based fMRI can vary considerably due to the heterogeneity of olfactory tasks and the shared neural substrates for sniffing and olfactory processing. [8, 9]. For instance, some fMRI studies have reported that odor stimulation leads to diminished activation within olfactory-related brain regions in individuals with olfactory disorders [7]. Conversely, another study reported increased responses and differential connectivity in the olfactory cortex in PTA patient [10]. Such discrepancies may, in part, be explained by differences in task design. In contrast, Resting-State fMRI (rs-fMRI) offers benefits that surpass those of task-based fMRI, as it does not involve premeditated stimulation or intentional movement, thereby avoiding the confounding effect of different tasks [11].

For the first time, Biswal et al. employed Seed-Based Analysis (SBA) to identify brain networks in a resting-state [12]. This method entails selecting Regions of Interest (ROIs) and computing the correlation between the average BOLD signal time course within these ROIs and the time courses of all other voxels across the brain. Numerous rs-fMRI studies have showcased the potential of SBA in pinpointing connectivity within a network in diseases [13, 14]. Beyond the SBA method, which determines the FC of the ROIs with other brain areas, the Independent Component Analysis (ICA) method does not necessitate an ROI. This method is a mathematical technique that maximizes statistical independence among its components. The ICA explores the voxel-to-voxel connection to extract patterns that represent the resting-state from mixed sources [15]. For rs-fMRI data, ICA can be utilized to spatially distinguish distinct functional connectivity networks in patients with olfactory loss [16]. Despite the differences in the two approaches, Rosazza et al. demonstrated that the results of SBA and ICA are significantly similar in a group of healthy subjects [17].

In this study, we used rs-fMRI to explore how functional connectivity patterns differ between individuals with PTA and healthy controls. Our main objective was to better understand how traumatic olfactory loss affects the brain's network organization. Accordingly, we applied two complementary approaches, ICA and SBA, allowing us to examine both general and olfactory-specific network alterations. We hypothesized that patients with PTA would show changed connectivity within key olfactory-related areas, such as the piriform cortex, orbitofrontal cortex, and insula. We also anticipated disruptions in higher-order regions, particularly the prefrontal cortex, which may reflect broader network-level consequences of olfactory loss. Given its regional specificity, we expected SBA to be more sensitive than ICA in detecting these changes. Additionally, we hypothesized that these connectivity alterations would be

associated with the severity of olfactory dysfunction, as measured by Threshold-Discrimination-Identification (TDI) scores. Exploring this relationship could provide insight into how functional brain changes relate to sensory performance in PTA. Overall, our aim was to provide a more complete picture of the neural changes associated with post-traumatic smell loss, with the hope of informing future clinical and therapeutic efforts.

Material and Methods

Participants

A total of 77 individuals participated in this retrospective study, comprising 43 Healthy Controls (HCs; mean age: 33±9.41 years; 26 males, 17 females) and 44 patients diagnosed with post-traumatic anosmia (PTA; mean age: 27.17±4.57 years; 25 males, 19 females). Participants were eligible for inclusion if they were between 20 and 45 years old, had olfactory dysfunction resulting from head trauma, and demonstrated confirmed impairment based on the Sniffin' Sticks test. Exclusion criteria included the presence of sinonasal disease, congenital anosmia, smoking, neurodegenerative disorders, and diabetes. All participants underwent otorhinolaryngological evaluations to rule out obstructive causes of olfactory dysfunction. Then, olfactory performance and rs-fMRI were performed.

Olfactory performance

Olfactory function was performed using the "Sniffin' Sticks" test battery (Burghart Messtechnik GmbH, Wedel, Germany). The test uses a pen like device to deliver the odor, which include specific tests for odor Threshold (T), odor Discrimination (D), and odor Identification (I). All tests were completed in agreement with the standardized computerized test protocol [18]. The odor detection threshold was assessed using serial dilutions of phenyl-ethyl alcohol following a 16-step staircase design and a three-alternative forced-choice paradigm. Odor discrimination was evaluated with 16 triplets of odorants, where two pens contained identical odors and the third carried a distinct one. For odor identification, 16 common scents were presented using a four-alternative forced-choice format. The T scores ranged from 1 to 16, while D and I score ranged from 0 to 16. The total scores from the threshold, discrimination, and identification subtests were summed to calculate the composite TDI score. Clinical diagnosis of anosmia was defined by a TDI score of 17 or less [19].

MRI acquisition

All participants underwent MRI using a 3T scanner system (Prisma, Siemens) at National Brain Mapping Lab (NBML), Tehran, Iran; using a 20-channel phased-array head coil. High-resolution T1-weighted images were acquired using a sagittal 3D magnetization prepared gradient rapid acquisition gradient echo sequence, aligned parallel to the anterior commissure–posterior commissure line. Imaging parameters were as follows: Repetition Time (TR) = 1800 ms; Echo Time (TE)= 3.53 ms; Inversion Time (TI) = 1100 ms; Field of View (FOV) = 256 mm; Voxel Size = 1×1×1 mm^3; Flip Angle = 7°; Number of Averages = 1 (in total, 160 contiguous slices of 1-mm thickness). The rs-fMRI data were acquired using a gradient-recalled, T2*-weighted whole-brain Echo-Planar Images (EPI) sequence, with the following parameters: TR = 2100 ms; TE = 30 ms; Flip Angle = 90°; FOV = 256 mm; Number of Slices = 36; Voxel Size = 3×3×3 mm^3. Individuals were instructed to close their eyes and not think of anything specific during the rs-fMRI scan.

fMRI data preprocessing

The rs-fMRI data were pre-processed with CONN toolbox (Connectivity Toolbox, https://www.nitrc.org/projects/conn) running through MatLab R2019a (MATLAB, http://www.mathworks.com/products/matlab,

MathWorks, Inc., Natick, MA) and SPM12 (SPM, https://www.fil.ion.ucl.ac.uk/spm/software/spm12) software. Data preprocessing included discarding the first three functional volumes to minimize initial image inhomogeneity, followed by slice-timing correction, image registration, and spatial normalization to Montreal Neurological Institute (MNI) space using segmentation-derived transformations. Subsequently, images were resampled to $3\times3\times3$ mm^3 and smoothed with an 8 mm Full Width at Half Maximum (FWHM). Anatomical data were resampled to 3 mm^3 voxels and functional data were aligned to the T1-weighted structural image and then to a Talairach atlas. The Artifact Removal Tools toolbox was utilized to identify artifacts that could potentially confound the BOLD signal in fMRI data. These artifacts, such as those related to White Matter (WM), Cerebrospinal Fluid (CSF), motion, scrubbing, and rest, were entered as covariates in a linear regression to eliminate their influence on the BOLD signal [20]. Once linear de-trending was completed, the images underwent a band-pass filtering process that eliminated temporal frequencies below 0.008 Hz and above 0.09 Hz. Additionally, motion regression was carried out to reduce the impact of motion and noise sources [21]. There were no statistically significant differences observed between the groups in terms of average realignment (P-value=0.6544) or framewise displacement (P-value=0.5278).

Seed-based analysis

We performed a seed-based functional connectivity analysis using the CONN toolbox and SPM12. For seed to voxel analyses, the pre-defined seeds were defined using WFU PickAtlas toolbox (https://www.nitrc.org/projects/wfu_pickatlas). All seeds were sphere in shape (5 mm radius, total 21 ROIs) and located at their center: piriform cortex (-22,0,14; 22,2,-12), insular cortex (-36,0,8; -30,18,6; -38,12,-2; -36,14,-8; -40,2,-14; 36,24,-2; 28,16,8; 40,12,-2), prefrontal cortex (-24,30,-10; 28,34,-12), anterior cingulate (20,48,-10; 10,36,-2; 6,36,20; -4,18,50; 6,28,38; 4,14,56; 42,34,28; 32,46,8; 44,40,0). Based on a previous publication [22], these ROIs in the olfactory network were defined by statistical localization. Then, a double check was carried out to ensure there were no overlapping voxels between the ROIs. First-level analysis was carried out by a general linear model to determine significant BOLD signal correlation with respect to time between the seeds and each voxel [23]. The resulting correlation coefficients were converted to z-scores using Fisher's Z transformation. Second-level analysis was performed using a two-sample t test to compare groups, with a False Discovery Rate (FDR) corrected P-value<0.01.

ROI to ROI approach was performed for investigating the detailed patterns of functional connectivity in whole-brain and olfactory networks. We used a total of 264 functional areas for brain network suggested by Power et al, [24] and a 21 pre-defined ROIs for olfactory network [22]. At the first level, all pairwise connections between ROIs on all subjects were examined for subsets of brain regions that have significant links to one another's seeds. The second-level between subject contrasts were determined by a two-sample t test with an FDR-corrected P-value<0.05.

Independent component analysis

Group-level spatial ICA was performed using the CONN toolbox, employing the FastICA algorithm to estimate independent spatial components and the GICA1 back-projection method to generate individual-level spatial maps [25, 26]. To detect resting-state networks, the number of components was set to 40 and dimensionality reduction was set to 64 as per CONN's default settings. Dual regression was used to identify the subject-specific contributions as part of the group level ICA. At the first level, ICA was applied to decompose the data and identify distinct patterns of FC for each individual subject. Subsequently,

spatial maps and their corresponding time courses were extracted. These component maps were then compiled for nonparametric analysis, enabling the assessment of statistical significance across groups. At the second level, group differences within each independent component were evaluated, with statistical significance determined using an FDR threshold of *P*-value<0.05.

Statistical analysis

The nonparametric Mann–Whitney test was employed using the Statistical Package for the Social Sciences (SPSS, version 23.0, IBM Corp., Armonk, NY, USA) to compare demographic data between the patient and healthy groups. The significance level for tests was set at *P*-value <0.05. To examine the significance of functional connectivity, each functional connectivity was analysed individually using Student's t distribution and its conversion into *P*-values. Further comparisons were made by testing functional connectivity within the network. Whole-brain FC analyses were conducted to investigate the relationship between changes in global efficiency, intrinsic connectivity, and alterations in olfactory performance. Results were thresholded at a *P*-value<0.05 with correction for multiple comparisons.

Results

Participants demography

The demographic characteristics of both PTA patients and HCs are presented in Table 1. No significant differences were observed between the groups in terms of gender (χ^2=0.549) or age (*P*-value=0.745). Among the PTA group, the mean duration of olfactory loss following head trauma was 9.12 months, ranging from 3 to 30 months. The mean TDI score was 12.39 in the PTA group and 36.31 in the HCs. According to the Mann–Whitney U test, patients with PTA had significantly lower TDI scores compared to healthy individuals (*P*-value<0.001).

Seed-to-voxel functional connectivity networks

Based on seed to voxel findings, alterations in functional connectivity were found in PTA group compared to the control group. PTA patients represented a higher the anterior cingulate cortex functional connectivity with the middle temporal gyrus and angular gyrus. They also exhibited increased connectivity between the left frontal cortex with middle temporal region and the posterior cingulate compared with healthy group (Table 2, Figure 1).

Table 1: Demographical and olfactory performance results

	Healthy Control	PTA	*P*-Value
Age (years)	33±9.41	27.17±4.57	0.745
Number; Gender (M/F)	43(26M, 17F)	44(25M, 19F)	0.549
Smell loss duration (months)	N.A	9.12±5.24	-
T score	11.27±2.11	1.23±1.12	<0.001
D score	11.97±1.7	5.78±2.23	<0.001
I score	13.06±1.36	5.32±3.12	<0.001
TDI score	36.31±2.62	12.39±4.68	<0.001

Data are presented as mean±SD, except for gender, which is reported as counts. *P*-values indicate statistically significant differences between the study groups. Independent-samples t-tests were used for continuous variables. The Chi-square test was used for categorical variables. M: Male; F: Female; T: Threshold; D: Discrimination; I: Identification; TDI: Threshold, Discrimination, and Identification; PTA: Post-Traumatic Anosmia; N.A: Not Applicable (This variable does not apply to healthy control participants).

ROI-to-ROI functional connectivity networks

The functional connectivity between anterior cingulate cortex and middle temporal gyrus and angular gyrus was higher in the PTA patient than HCs. In addition, functional connectivity between left insula with a supramarginal gyrus and thalamus and also right insula with right middle temporal and frontal parietal cortex was higher in PTA patient comparison to HCs. The PTA patient group represented a higher piriform cortex functional connectivity with the thalamus. Furthermore, the functional connectivity between the prefrontal cortex with para cingulate region, anterior cingulate cortex, inferior temporal, left angular gyrus,

Table 2: Comparison of seed-based functional connectivity networks in the study subjects

Seed (ROI)	MNI			Region	Voxel size	P-FDR
	X	Y	Z			
Anterior cingulate cortex	+64	-22	-10	Rt middle temporal gyrus	269	0.007692
Prefrontal	-14	+50	+30	Lt frontal pole	2358	0.00001
	+58	+02	-34	Rt middle temporal gyrus	454	0.000206
	-02	-18	+36	Lt post cingulate gyrus	317	0.001713

The result shows a statistically significant cluster (*P*-FDR<0.05). All coordinates are given in Montreal Neurological Institute (MNI) space. Rt: Right, Lt: Left, FDR: False Discovery Rate

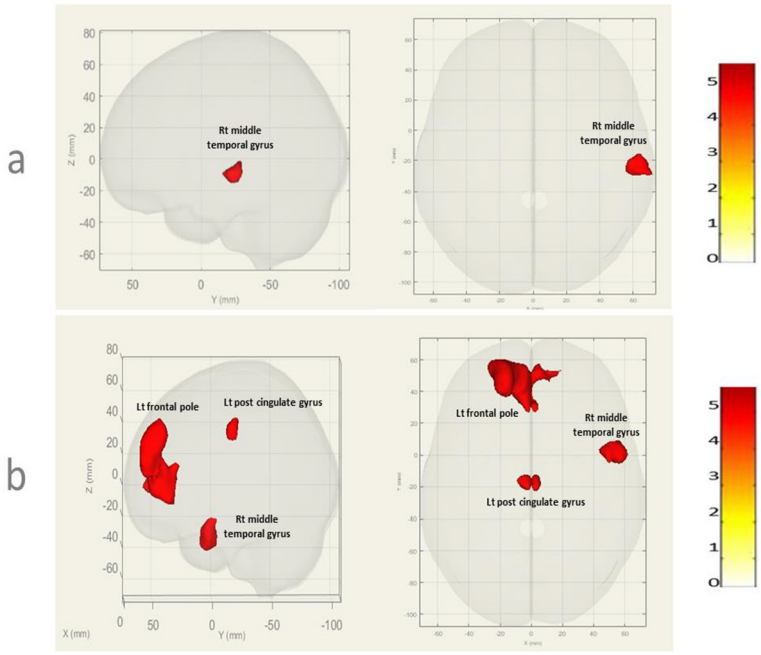

Figure 1: Seed-based functional connectivity networks in Post-Traumatic Anosmia (PTA) vs healthy controls. Regions that showed increased functional connectivity in PTA patients. The results were obtained using a seed-based analysis method with the anterior cingulate cortex (**a**) and prefrontal cortex (**b**) as seeds. Red indicates a greater positive connectivity. (Rt: Right, LT: Left)

middle temporal, praecuneus cortex, and right temporal pole was higher in anosmia patient compare to HCs (Table 3, Figure 2).

ICA functional connectivity networks

The group-ICA using CONN was used to discover diverse brain networks in rs-fMRI data to verify alteration of functional connectivity of PTA group compared to the control group. In the ICA analysis, we calculated 40 independent components to identify the brain networks associated with each ICA component. As a result of ICA analysis thirteen resting-state brain networks were acquired, including right frontal pole, left cerebellum crus2, right cerebellum 8, right putamen, anterior cingulate gyrus, right postcentral gyrus, left orbitofrontal cortex, left lateral occipital cortex (superior division), supramarginal gyrus, right lateral occipital cortex (superior division), right cerebellum crus, left lingual gyrus and left amygdala (Table 4, Figure 3).

Correlations in networks and TDI score

In PTA patients, the global efficiency of the whole brain network was significantly associated with the TDI score (R2=0.63, *P*-value=0.003), and intrinsic connectivity of the whole brain network was also significantly correlated with the TDI score (R2=0.66, *P*-value =0.001). Also, after controlling for smell loss duration, the association was remained significant for global efficiency (R2=0.70, *P*-value<0.001), and intrinsic connectivity (R2=0.73, *P*-value<0.001) (Figure 4). There was no significant association between the network

Table 3: Comparison functional connectivity in subjects using the region of interest analysis

Seed (ROI)	Target	Beta	T (75)	*P*-FDR
Rt anterior cingulate cortex	Rt middle temporal gyrus	-0.13	-3.84	0.021
	Rt angular gyrus	-0.14	-3.72	0.030
Lt insula	Rt supramarginal gyrus	0.22	4.23	<0.001
	Lt thalamus	-0.15	-3.78	<0.001
Rt insula	Rt frontal parietal cortex	0.20	3.72	<0.001
	Rt middle temporal gyrus	0.17	3.70	0.013
Lt piriform	Lt thalamus	-0.18	-4.59	0.031
Rt prefrontal	Lt paracingulate	0.20	4.28	0.042
	Lt anterior cingulate gyrus	0.19	4.08	<0.001
	Lt inferior temporal gurus	0.19	4.08	0.024
	Brain stem	-0.13	-3.61	0.027
	Lt network language	0.20	3.59	0.036
	Lt Angular gyrus	0.19	3.33	<0.001
	Lt Middle temporal gyrus	0.21	3.33	0.022
	Rt inferior temporal gyrus	-0.16	-3.26	0.021
	Rt precuneus cortex	0.16	3.15	0.030
	Rt temporal pole	0.14	3.10	<0.001
	Rt network dorsal attention	-0.15	-3.10	<0.001

The result shows a statistically significant cluster (*P*-FDR<0.05). Rt: Right, Lt: Left, FDR; False Discovery Rate

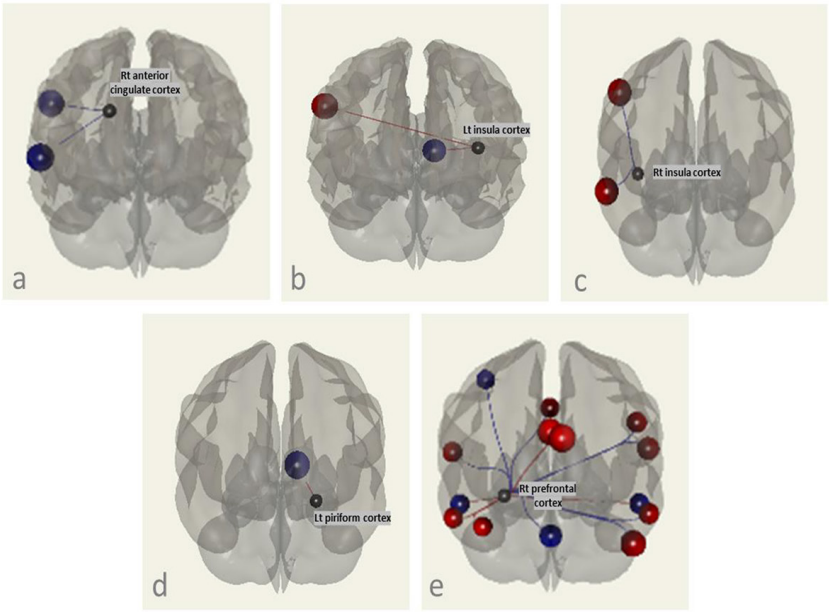

Figure 2: Region of interest functional connectivity networks in post-traumatic anosmia vs healthy controls. Regions show higher functional connectivity in PTA patient compare to HCs. The results were acquired using a ROI-to-ROI analysis method with ROIs of (**a**) Right anterior cingulate cortex; (**b**) Left insula cortex; (**c**) Right insula cortex; (**d**) Left piriform cortex; (**e**) Right prefrontal cortex. (ROI: Region of Interest, PTA: Post-Traumatic Anosmia, HCs: Healthy Controls, Rt: Right, Lt: Left)

Table 4: Comparison functional connectivity in subjects using group independent component analysis

Brain area	MNI			Voxel size	*P*-FDR
	X	Y	Z		
Rt frontal pole	36	36	14	369	0.003718
Lt cerebellum crus2	-20	-78	-36	1160	0.000000
Rt cerebellum 8	24	-60	-58	280	0.016308
Rt putamen	28	0	-12	224	0.006675
Rt anterior cingulate gyrus	10	24	18	2158	0.000000
Rt postcentral gyrus	18	-30	80	95	0.014441
Lt orbitofrontal cortex	-12	6	-16	262	0.011585
Lt lateral occipital gyrus (superior division)	-50	-80	30	911	0.000001
Rt supramarginal gyrus	68	-40	24	294	0.003908
Rt lateral Occipital gyrus (superior division)	34	-72	14	1101	0.000000
Rt cerebellum crus1	50	-76	-28	346	0.004143
Lt lingual gyrus	-20	-30	-10	848	0.000002
Lt amygdala	-32	0	-18	310	0.003688

The result shows a statistically significant cluster (*P*-FDR<0.05). All coordinates are given in Montreal Neurological Institute (MNI) space. FDR: False Discovery Rate, Rt: Right, Lt: Left

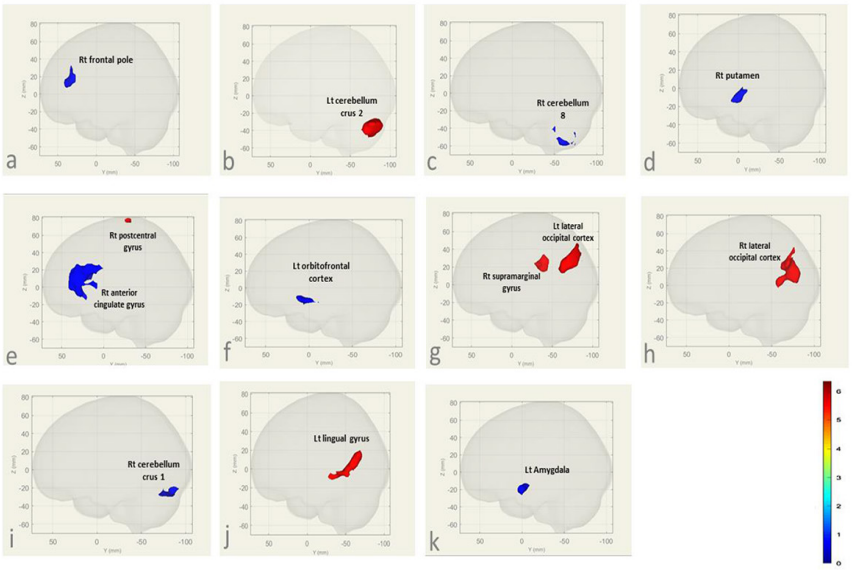

Figure 3: Characteristics of functional connectivity networks using independent component analysis. **a**) Right frontal pole; **b**) Left cerebellum crus2; **c**) Right cerebellum 8; **d**) Right putamen; **e**) Right anterior cingulate gyrus and right postcentral gyrus; **f**) Left orbitofrontal cortex; **g**) Left lateral occipital cortex (superior division) and right supramarginal gyrus; **h**) Right lateral occipital cortex (superior division); **i**) Right cerebellum crus1; **j**) Left lingual gyrus; **k**) Left Amygdala

parameters and other clinical variables.

Discussion

Our study investigated the neural alterations in post-traumatic anosmia patients through resting-state fMRI. The findings indicated that PTA patients had lower olfactory function scores and heightened functional connectivity in specific brain regions compared to healthy controls. Notably, both seed-based and independent component analyses revealed increased functional connectivity in higher-order areas beyond the olfactory cortex. These results imply that olfactory impairment induced by head trauma is marked by changes in functional connectivity, which may serve as a potential neural marker for PTA. Furthermore, the correlation between the global efficiency of the entire brain network and olfactory function emphasizes the broad impact of PTA on overall brain function.

The initial processing of olfactory neural signals beyond the olfactory bulb occurs in the olfactory cortex, consisting of several brain regions, including the anterior olfactory nucleus, the olfactory tubercle, the piriform cortex, the amygdala, and the entorhinal cortex. Each of these regions receives direct, monosynaptic input from the olfactory bulb [27]. The piriform cortex, the largest structure within the olfactory cortex, can be anatomically and functionally divided into the anterior and posterior piriform cortices. It is suggested that the anterior piriform cortex encodes the identity of odorants, while the posterior piriform cortex may encode their quality [28]. Beyond the olfactory cortex, olfactory projections extend to the orbitofrontal cortex and the anterior insula. The orbitofrontal cortex is involved in odor discrimination, identification, and memory. Notably, only the right orbitofrontal cortex is engaged in conscious olfaction [27]. Conversely, the anterior insula is considered a cognitive-evaluative area, often displaying high activation in studies requiring a task to be performed while exposed to an olfactory

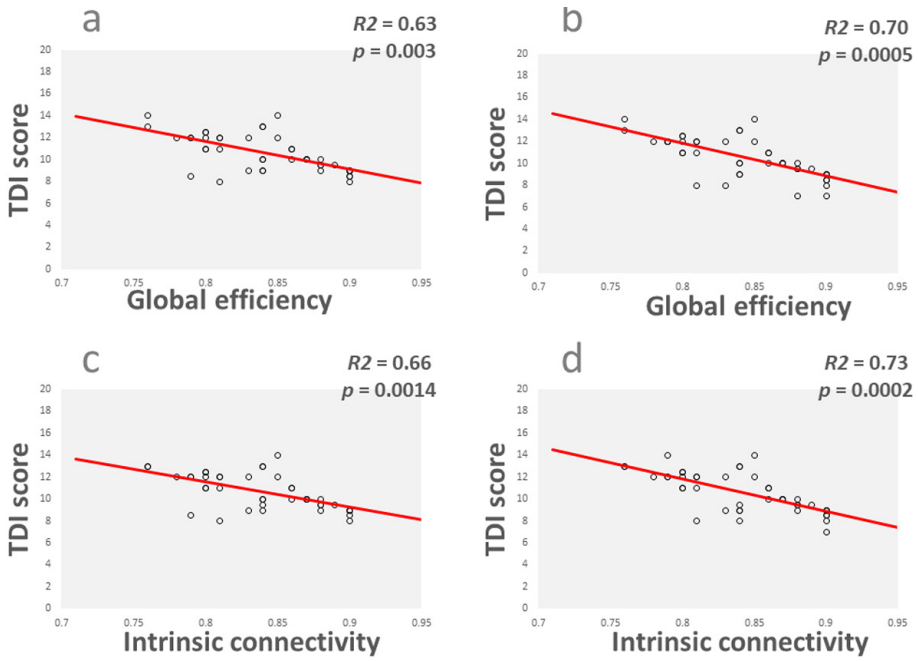

Figure 4: Correlation between network parameters and TDI score for post-traumatic anosmia patients. Scatter plots show linear relationships between TDI score, network parameters, and smell loss duration. R-squared and *P*-values of whole regression model are presented. (**a**) Association between global efficiency and TDI score; (**b**) Association between global efficiency and TDI score, after smell duration controlled; (**c**) Association between intrinsic connectivity and TDI score; (**b**) Association between intrinsic connectivity and TDI score, after smell duration controlled. (TDI: Threshold-Discrimination-Identification)

stimulus [22]. This comprehensive understanding of olfactory neural processing pathways offers valuable insights into the functioning of the olfactory system.

The SBA findings indicate a compensatory mechanism in the brains of anosmia patients, where other areas are utilized to offset damage in affected regions. These results may suggest that this compensatory mechanism, which relies on engaging different brain regions, is significant in understanding traumatic olfactory dysfunction, as previously proposed in various neurodegenerative diseases [29, 30]. A prior study on traumatic anosmia revealed that a compensatory mechanism has been established within the brain [31]. Substantial evidence supports the brain's plasticity following the formation of pathological lesions [30]. Additionally, this plasticity has been confirmed after head injuries associated with olfactory dysfunction [32, 33]. Previous research indicated varying changes in the functional connectivity of brain networks in PTA patients, particularly involving the prefrontal areas, the left inferior frontal gyrus, and the left premotor cortex [34-36]. Moreover, regarding anosmia, increased connectivity at the cognitive level of the olfactory system has been demonstrated. The fundamental mechanisms underpinning olfactory system plasticity remain a topic of debate [34, 37]. Structural analyses have shown an increase in gray matter volume in the brains of those with traumatic anosmia [31], providing further evidence of the brain's compensatory mechanisms.

Our study does not fully align with previous research, which has primarily focused on the onset of olfactory disorders in the early stages

of neurodegenerative diseases [23, 38]. Using odor-stimulated, task-based fMRI, earlier studies reported decreased activation in the olfactory region of the brain [38, 39]. The first study on functional connectivity in task-based fMRI demonstrated reduced connectivity in both olfactory and non-olfactory networks [40]. However, in the present study, we observed increased functional connectivity in certain regions compared to the control group. These discrepancies may be attributed to methodological differences. For instance, while the previous studies employed task-based fMRI [38-40], our analysis used rs-fMRI to assess whole-brain functional connectivity.

In a previous study on hyposmia subjects in the resting-state, it was concluded that there was activation between the piriform cortex and the inferior temporal region [39]. Similarly, in our study, we observed activity in these same regions. Another study conducted on traumatic anosmia using rs-fMRI found increased functional connectivity in the olfactory region of the patient group compared to healthy controls. Additionally, this study reported increased functional connectivity in both the visual and motor cortices of the patient group [39]. In our study, group comparisons from seed analysis also revealed increased functional connectivity in the patient group compared to the healthy group. Specifically, activation was observed in the middle temporal gyrus with the anterior cingulate region, as well as in the left frontal pole, middle temporal gyrus, and posterior cingulate gyrus with the prefrontal region. Furthermore, increased functional connectivity was noted between the anterior cingulate cortex and the left occipital pole, and between the insula and lateral occipital cortex, indicating enhanced connectivity in the visual cortex of the patient group.

ICA is well-suited for identifying functionally connected brain areas without the need to predefine the hemodynamic response function or the design matrix. In this study, ICA successfully detected a functional network that included the olfactory cortex (specifically the posterior piriform cortex) and its primary projections, such as the insula, orbitofrontal cortex, and thalamus. This network's activity aligned temporally with the olfactory fMRI design. Using a group-ICA approach, several brain areas (detailed in Table 4) in individuals with traumatic anosmia showed higher activity compared to the control group, suggesting increased regional activity in anosmia patients. In related ICA analysis of individuals with congenital anosmia, heightened activity was observed in the insula and piriform cortex compared to healthy controls, indicating functional connectivity changes in olfactory regions [41]. Similarly, a study on Parkinson's patients reported ICA-detected neuroactive regions within the olfactory network, including the posterior piriform cortex, insula, orbitofrontal cortex, and thalamus [23].

This study has several limitations. First, the sample size was relatively small, which may limit the generalizability of the findings. Second, although there were no significant differences in age or gender between the PTA and control groups, participants were not explicitly matched based on potential confounders such as age, gender, or medication use. Due to technical constraints, it was not feasible to include these variables as covariates in the group-level analyses. Nevertheless, the lack of significant demographic differences reduces the likelihood of substantial confounding effects. Third, the use of only two analytical methods (ICA and SBA) may restrict the depth of interpretation. Fourth, while rs-fMRI provides valuable insights, it does not capture dynamic or task-specific neural changes, and its correlational nature limits causal inference between connectivity patterns and olfactory function. Future studies should consider increasing the sample size, incorporating additional analytical techniques, such as graph-theoretical approaches, and applying longitudinal designs to better characterize the progression of brain connectivity alterations in PTA.

Conclusion

The findings suggest that ICA of rs-fMRI provides evidence that olfactory impairment in PTA is linked to significantly reduced recruitment of the olfactory network. Moreover, our seed-based analysis revealed that distinct brain regions were exclusively associated with different aspects of traumatic anosmia, while some areas showed activation in the control group. Ultimately, using rs-fMRI to investigate functional connectivity differences across regions may offer a potential method for detecting olfactory dysfunction in a resting-state.

Acknowledgment

Authors would like to acknowledge the National Brain Mapping Lab of Iran, for MRI data acquisition.

Authors' Contribution

A. Zare-Sadeghi contributed to the conception, design, and project administration of the study. A. Rezaeyan & F. Shahi Moridi were responsible for data curation, formal analysis, methodology, and writing of the original draft. SK. Kamrava & MB. Shiran critically revised the manuscript for important intellectual content. All authors read, revised, and approved the final version of the manuscript.

Ethical Approval

The Ethics Committee of Iran University of Medical Sciences approved the study protocol (Ethical code: IR.IUMS.FMD.REC.1400.433).

Informed Consent

The authors declare that they obtained a written informed consent from the patients and/or volunteers included in the article and that this report does not contain any personal information that could lead to their identification.

Funding

This research was supported by grant [19541] from the Iran University of Medical Sciences.

Conflict of Interest

None

References

1. Croy I, Nordin S, Hummel T. Olfactory disorders and quality of life--an updated review. *Chem Senses.* 2014;**39**(3):185-94. doi: 10.1093/chemse/bjt072. PubMed PMID: 24429163.
2. Proskynitopoulos PJ, Stippler M, Kasper EM. Post-traumatic anosmia in patients with mild traumatic brain injury (mTBI): A systematic and illustrated review. *Surg Neurol Int.* 2016;**7**(Suppl 10):S263-75. doi: 10.4103/2152-7806.181981. PubMed PMID: 27213113. PubMed PMCID: PMC4866055.
3. Howell J, Costanzo RM, Reiter ER. Head trauma and olfactory function. *World J Otorhinolaryngol Head Neck Surg.* 2018;**4**(1):39-45. doi: 10.1016/j.wjorl.2018.02.001. PubMed PMID: 30035260. PubMed PMCID: PMC6051255.
4. Su B, Bleier B, Wei Y, Wu D. Clinical Implications of Psychophysical Olfactory Testing: Assessment, Diagnosis, and Treatment Outcome. *Front Neurosci.* 2021;**15**:646956. doi: 10.3389/fnins.2021.646956. PubMed PMID: 33815048. PubMed PMCID: PMC8012732.
5. Saltagi AK, Saltagi MZ, Nag AK, Wu AW, Higgins TS, Knisely A, et al. Diagnosis of Anosmia and Hyposmia: A Systematic Review. *Allergy Rhinol (Providence).* 2021;**12**:21526567211026568. doi: 10.1177/21526567211026568. PubMed PMID: 34285823. PubMed PMCID: PMC8264728.
6. Yousem DM, Williams SC, Howard RO, Andrew C, Simmons A, Allin M, et al. Functional MR imaging during odor stimulation: preliminary data. *Radiology.* 1997;**204**(3):833-8. doi: 10.1148/radiology.204.3.9280268. PubMed PMID: 9280268.
7. Moon WJ, Park M, Hwang M, Kim JK. Functional MRI as an Objective Measure of Olfaction Deficit in Patients with Traumatic Anosmia. *AJNR Am J Neuroradiol.* 2018;**39**(12):2320-5. doi: 10.3174/ajnr.A5873. PubMed PMID: 30409849. PubMed PMCID: PMC7655384.
8. Vedaei F, Oghabian MA, Firouznia K, Harirchian MH, Lotfi Y, Fakhri M. The human olfactory system: Cortical brain mapping using fMRI. *Iran J Radiol.* 2017;**14**(2):e16250. doi: 10.5812/iranjradiol.16250.
9. Yunpeng Z, Han P, Joshi A, Hummel T. Individual variability of olfactory fMRI in normosmia and ol-

factory dysfunction. *Eur Arch Otorhinolaryngol*. 2021;**278**(2):379-87. doi: 10.1007/s00405-020-06233-y. PubMed PMID: 32803385. PubMed PMCID: PMC7826297.

10. Pellegrino R, Farruggia MC, Small DM, Veldhuizen MG. Post-traumatic olfactory loss and brain response beyond olfactory cortex. *Sci Rep.* 2021;**11**(1):4043. doi: 10.1038/s41598-021-83621-2. PubMed PMID: 33597627. PubMed PMCID: PMC7889874.
11. Park M, Chung J, Kim JK, Jeong Y, Moon WJ. Altered Functional Brain Networks in Patients with Traumatic Anosmia: Resting-State Functional MRI Based on Graph Theoretical Analysis. *Korean J Radiol.* 2019;**20**(11):1536-45. doi: 10.3348/kjr.2019.0104. PubMed PMID: 31606958. PubMed PMCID: PMC6791817.
12. Biswal B, Yetkin FZ, Haughton VM, Hyde JS. Functional connectivity in the motor cortex of resting human brain using echo-planar MRI. *Magn Reson Med.* 1995;**34**(4):537-41. doi: 10.1002/mrm.1910340409. PubMed PMID: 8524021.
13. Palacios EM, Sala-Llonch R, Junque C, Roig T, Tormos JM, Bargallo N, Vendrell P. Resting-state functional magnetic resonance imaging activity and connectivity and cognitive outcome in traumatic brain injury. *JAMA Neurol.* 2013;**70**(7):845-51. doi: 10.1001/jamaneurol.2013.38. PubMed PMID: 23689958.
14. Palacios EM, Yuh EL, Chang YS, Yue JK, Schnyer DM, Okonkwo DO, et al. Resting-State Functional Connectivity Alterations Associated with Six-Month Outcomes in Mild Traumatic Brain Injury. *J Neurotrauma*. 2017;**34**(8):1546-57. doi: 10.1089/neu.2016.4752. PubMed PMID: 28085565. PubMed PMCID: PMC5397233.
15. Beckmann CF, DeLuca M, Devlin JT, Smith SM. Investigations into resting-state connectivity using independent component analysis. *Philos Trans R Soc Lond B Biol Sci*. 2005;**360**(1457):1001-13. doi: 10.1098/rstb.2005.1634. PubMed PMID: 16087444. PubMed PMCID: PMC1854918.
16. Kollndorfer K, Jakab A, Mueller CA, Trattnig S, Schöpf V. Effects of chronic peripheral olfactory loss on functional brain networks. *Neuroscience*. 2015;**310**:589-99. doi: 10.1016/j.neuroscience.2015.09.045. PubMed PMID: 26415766.
17. Rosazza C, Minati L, Ghielmetti F, Mandelli ML, Bruzzone MG. Functional connectivity during resting-state functional MR imaging: study of the correspondence between independent component analysis and region-of-interest-based methods. *AJNR Am J Neuroradiol*. 2012;**33**(1):180-7. doi: 10.3174/ajnr.A2733. PubMed PMID: 21998099. PubMed PMCID: PMC7966157.
18. Hummel C, Zucco GM, Iannilli E, Maboshe W, Landis BN, Hummel T. OLAF: standardization of international olfactory tests. *Eur Arch Otorhinolaryngol.* 2012;**269**(3):871-80. doi: 10.1007/s00405-011-1770-0. PubMed PMID: 21935630.
19. Lötsch J, Hummel T. Clinical Usefulness of Self-Rated Olfactory Performance-A Data Science-Based Assessment of 6000 Patients. *Chem Senses.* 2019;**44**(6):357-64. doi: 10.1093/chemse/bjz029. PubMed PMID: 31077277.
20. Behzadi Y, Restom K, Liau J, Liu TT. A component based noise correction method (CompCor) for BOLD and perfusion based fMRI. *Neuroimage.* 2007;**37**(1):90-101. doi: 10.1016/j.neuroimage.2007.04.042. PubMed PMID: 17560126. PubMed PMCID: PMC2214855.
21. Nieto-Castanon A. Handbook of functional connectivity magnetic resonance imaging methods in CONN. Hilbert Press; 2020.
22. Seubert J, Freiherr J, Djordjevic J, Lundström JN. Statistical localization of human olfactory cortex. *Neuroimage*. 2013;**66**:333-42. doi: 10.1016/j.neuroimage.2012.10.030. PubMed PMID: 23103688.
23. Georgiopoulos C, Witt ST, Haller S, Dizdar N, Zachrisson H, Engström M, Larsson EM. A study of neural activity and functional connectivity within the olfactory brain network in Parkinson's disease. *Neuroimage Clin.* 2019;**23**:101946. doi: 10.1016/j.nicl.2019.101946. PubMed PMID: 31491835. PubMed PMCID: PMC6661283.
24. Power JD, Cohen AL, Nelson SM, Wig GS, Barnes KA, Church JA, et al. Functional network organization of the human brain. *Neuron*. 2011;**72**(4):665-78. doi: 10.1016/j.neuron.2011.09.006. PubMed PMID: 22099467. PubMed PMCID: PMC3222858.
25. Calhoun VD, Liu J, Adali T. A review of group ICA for fMRI data and ICA for joint inference of imaging, genetic, and ERP data. *Neuroimage.* 2009;**45**(1 Suppl):S163-72. doi: 10.1016/j.neuroimage.2008.10.057. PubMed PMID: 19059344. PubMed PMCID: PMC2651152.
26. Calhoun VD, Adali T, Pearlson GD, Pekar JJ. A method for making group inferences from functional MRI data using independent component analysis. *Hum Brain Mapp*. 2001;**14**(3):140-51. doi: 10.1002/hbm.1048. PubMed PMID: 11559959. PubMed PMCID: PMC6871952.
27. Gottfried JA. Central mechanisms of odour object perception. *Nat Rev Neurosci.* 2010;**11**(9):628-41. doi: 10.1038/nrn2883. PubMed PMID: 20700142. PubMed PMCID: PMC3722866.
28. Van Hartevelt TJ, Kringelbach ML. The Olfactory

System. Chapter 34. In: Mai JK, Paxinos G, editors. The Human Nervous System (Third Edition). San Diego: Academic Press; 2012. p. 1219-38.

29. Hosseini SF, Farhadi M, Alizadeh R, Ghanbari H, Maleki S, Zare-Sadeghi A, Kamrava SK. The brain functional connectivity alterations in traumatic patients with olfactory disorder after low-level laser therapy demonstrated by fMRI. *Neuroradiol J.* 2023;**36**(6):716-27. doi: 10.1177/19714009231188589. PubMed PMID: 37533379. PubMed PMCID: PMC10649526.
30. Bettus G, Guedj E, Joyeux F, Confort-Gouny S, Soulier E, Laguitton V, et al. Decreased basal fMRI functional connectivity in epileptogenic networks and contralateral compensatory mechanisms. *Hum Brain Mapp*. 2009;**30**(5):1580-91. doi: 10.1002/hbm.20625. PubMed PMID: 18661506. PubMed PMCID: PMC6870867.
31. Han P, Winkler N, Hummel C, Hähner A, Gerber J, Hummel T. Alterations of Brain Gray Matter Density and Olfactory Bulb Volume in Patients with Olfactory Loss after Traumatic Brain Injury. *J Neurotrauma*. 2018;**35**(22):2632-40. doi: 10.1089/neu.2017.5393. PubMed PMID: 29699465.
32. Rezaeyan A, Asadi S, Kamrava SK, Zare-Sadeghi A. Brain structural analysis in patients with post-traumatic anosmia: Voxel-based and surface-based morphometry. *J Neuroradiol.* 2023;**50**(5):482-91. doi: 10.1016/j.neurad.2022.11.005. PubMed PMID: 36610937.
33. Rezaeyan A, Asadi S, Kamrava SK, Khoei S, Zare-Sadeghi A. Reorganizing brain structure through olfactory training in post-traumatic smell impairment: An MRI study. *J Neuroradiol.* 2022;**49**(4):333-42. doi: 10.1016/j.neurad.2021.04.035. PubMed PMID: 33957160.
34. Kollndorfer K, Kowalczyk K, Hoche E, Mueller CA, Pollak M, Trattnig S, Schöpf V. Recovery of olfactory function induces neuroplasticity effects in patients with smell loss. *Neural Plast.* 2014;**2014**:140419. doi: 10.1155/2014/140419. PubMed PMID: 25544900. PubMed PMCID: PMC4269319.
35. Kaheni H, Shiran MB, Kamrava SK, Zare-Sadeghi A. Intra and inter-regional functional connectivity of the human brain due to Task-Evoked fMRI Data classification through CNN & LSTM. *J Neuroradiol.* 2024;**51**(4):101188. doi: 10.1016/j.neurad.2024.02.006. PubMed PMID: 38408721.
36. Rezaeyan A, Asadi S, Kamrava SK, Zare-Sadeghi A. Olfactory training affects the correlation between brain structure and functional connectivity. *Neuroradiol J.* 2025;**38**(4):450-63. doi: 10.1177/19714009241303129. PubMed PMID: 39626165. PubMed PMCID: PMC11615909.
37. Bende M, Nordin S. Perceptual learning in olfaction: professional wine tasters versus controls. *Physiol Behav*. 1997;**62**(5):1065-70. doi: 10.1016/s0031-9384(97)00251-5. PubMed PMID: 9333201.
38. Wang J, Eslinger PJ, Doty RL, Zimmerman EK, Grunfeld R, Sun X, et al. Olfactory deficit detected by fMRI in early Alzheimer's disease. *Brain Res.* 2010;**1357**:184-94. doi: 10.1016/j.brainres.2010.08.018. PubMed PMID: 20709038. PubMed PMCID: PMC3515873.
39. Henkin RI, Levy LM. Functional MRI of congenital hyposmia: brain activation to odors and imagination of odors and tastes. *J Comput Assist Tomogr.* 2002;**26**(1):39-61. doi: 10.1097/00004728-200201000-00008. PubMed PMID: 11801904.
40. Kollndorfer K, Fischmeister FP, Kowalczyk K, Hoche E, Mueller CA, Trattnig S, Schöpf V. Olfactory training induces changes in regional functional connectivity in patients with long-term smell loss. *Neuroimage Clin.* 2015;**9**:401-10. doi: 10.1016/j.nicl.2015.09.004. PubMed PMID: 26594622. PubMed PMCID: PMC4590718.
41. Peter MG, Fransson P, Mårtensson G, Postma EM, Nordin LE, Westman E, et al. Normal Olfactory Functional Connectivity Despite Lifelong Absence of Olfactory Experiences. *Cereb Cortex.* 2021;**31**(1):159-68. doi: 10.1093/cercor/bhaa217. PubMed PMID: 32810869. PubMed PMCID: PMC7727390.